THE EFFECTS OF TAPER SIZE ON THE FRACTURE RESISTANCE OF ROOT SECTIONS

A THESIS
SUBMITTED TO THE FACULTY OF THE GRADUATE SCHOOL OF THE UNIVERSITY OF MINNESOTA
BY

TOM HAI-TAM NGUY

IN PARTIAL FULFILLMENT OF THE REQUIREMENTS FOR THE DEGREE OF MASTER OF SCIENCE

SCOTT B. MCCLANAHAN

ADVISOR

AUGUST 2012

ACKNOWLEDGEMENTS

The following people have played an essential role toward my growth in the field of endodontics; with sincere gratitude and appreciation:

Dr. McClanahan- You continued to push me and made sure that I will become the best endodontist that I can be

Dr. Baisden- Your enthusiasm and support made it easier when the going gets tough

Dr. Bowles- The wealth of knowledge that you possess is truly amazing

Drs. Spitzmueller, Baumgartner, Edmunds, Zucker, Doyle- Your continued dedication to the program is part of the reason why I was able to succeed as a resident

Residents- I will always cherish our camaraderie through both the good and bad times

Assistants and Staff- All of you made my life easier and I will always appreciate all the support that you have given me

DEDICATION

To my family, for their support over the past two years and always believing in me

To my close friend, for your continued support and encouragement when things got tough

TABLE OF CONTENTS

LIST OF FIGURES

LIST OF TABLES

Introduction

The inception of endodontics as a field of dentistry followed an interesting course; the concept of an endodontic infection was first introduced as the “tooth worm” theory affecting the hollow portion inside the tooth. These creatures were thought to cause much pain and discomfort to their victims by constantly gnawing at the tooth structure (Cruse et al., 1980). Following this origin, many approaches were taken to effectively remove the source of endodontic infection and obturate the space with various materials such as lead and gold. The methods of pulpal removal historically included utilization of a red-hot probe, boiling oil, arsenic, and oil of cinnamon. The focal infection theory proposed by Dr. William Hunter, which largely favored dental extractions over pulpal therapy, was a significant setback to the field of endodontics. This theory supported the concept that dental infections are responsible for many widespread maladies through the bloodstream; as a result, further advancements in endodontics were not made until this theory was eventually disproven. Subsequent hallmarks in the field of endodontics are many, but the introduction of Nickel Titanium alloys (NiTi) stands out. The superelastic nature of NiTi revolutionized are many, endodontic treatment by allowing dental practitioners to instrument teeth with difficult anatomy and since then a wide range of NiTi endodontic file systems have been introduced to the market. Apart from its physical properties, elements of file design such as size and taper also confer clinical significance. While larger tapered instruments remove more dentin and make tooth debridement and irrigation easier, it can compromise the tooth. A balance must be established

between sufficient removal of infected tissue and preservation of remaining tooth structure. It is of the utmost importance for root canal therapy to be as effective as it is conservative. In order to elucidate the association between file design and root fractures, the aim of this study was to investigate the differences between larger file taper and its effect on the fracture resistance of root sections.

Review of Literature

History of instrumentation

The first endodontic instrument was first described by the father of modern dentistry, Pierre Fauchard, as a small pin used in pulpal extirpation. The predecessor to the modern endodontic file took form as a four sided broach that was fabricated by Edwin Maynard filing of a watch spring in 1838 (Grossman et al., 1976). The use of an instrument in a rotary handpiece was first developed by William H. Rollins, but it was not until the invention of the Canal Finder System in 1984 by Guy Levy that gave rise to a new era in rotary instrumentation (Levy 1984). The last decade has witnessed an explosion in the designs of rotary files and currently, there are over 20 different types of NiTi systems in the market (Vaudt 2007).

Concepts of instrumentation

Regardless of the files type or designs, the goal of endodontic therapy remains the same, which is removal of bacteria. Kakehashi et al (1965) that they are the primary etiology of endodontic infections. Additionally, Moller et al (1981) showed that these pathogens were typically part of the oral flora and their byproducts were capable of progressing beyond the root canal system and causing inflammation in the periapical tissues (Schonfeld et al., 1982). One method that facilitates the effective removal of these microorganisms is through mechanical means as shown by Siquiera et al (1999) that instrumentation and

plain saline irrigation of the root canal system can remove up to 90% of the bacteria present in root canals. For the remaining 10% of the pathogens, the use of chemical solutions such as 6% NaOCl is required to achieve complete disinfection of the root canal system and this is the only irrigant with the capability of removing biofilms (Clegg 2002).

It was also found that larger apical preparations had an effect on bacterial reduction, as 100% of canals instrumented to a Lightspeed file size #80-#100 was rendered bacteria free when compared to smaller file sizes (Card et al., 2002). The development of Nickel Titanium (NiTi) by W.F. Buehler at the Naval Ordinance Laboratory in Silver Springs, Maryland in the 1960's saw its gradual introduction into dentistry. Nicknamed "Nitinol", the alloy consisted of 56% nickel and 44% titanium by weight.

The superelastic nature of NiTi along with its shape memory can be attributed to the metal's atomic bonding. This enabled NiTi to undergo a transformation from a cubic lattice (Austenitic phase) to a hexagonal lattice configuration (Martensitic phase) and vice versa through heating and cooling. The start and finish of this martensitic transformation (Martensite start or Ms and Martensite finish point or Mf) gave rise to its shape memory characteristic (Wang et al., 1972). Another process by which this transformation occurs was through stress induction during root canal preparation that also took advantage of the superelasticity behavior of the material. According to Thompson (1999), "the rate of increase stress leveled off despite added strain" during this stage and springback occurred when the stress was decreased or stopped. An additional

feature of NiTi when subjected to stress was its ability to undergo fully reversible deformation up to 8% strain when compared to the 0.2-0.5% in stainless steel (McKelvey et al. 1999, Rasmussen 2001). When compared to stainless steel handfiles, in terms of torsional and bending properties, NiTi files had 2-3 times more elastic flexibility and were superior in its resistance to torsional fracture (Walia 1988). Despite advances in instrument designs, up to 35% of the surface area of root canals still remained uninstrumented (Peters 2001). This meant that the bulk of canal instrumentation continues to rely on irrigants to achieve the mechanical and biological objectives of cleaning and shaping root canals as described by Schilder in 1974 along with mechanical debridement.

Advantages of rotary

The use of rotary instrumentation enhances tactile awareness by removing canal obstructions in the coronal and middle third of the root. It has also been determined that using hand instrumentation methods with the first file that binds and working it three sizes up is ineffective since in 25% of the specimens, there was no engagement of the instrument against the canal wall at working length (Wu, 2002). It was advocated to instead perform adequate apical enlargement to enable effective filing and irrigation (Wu 2002).

The technique for most rotary instrumentation utilized the concept of crown down. Also called the pressureless crown down technique, it was first described by Marshall et al. in 1980 and involved starting with larger instruments coronally and progressively moving apically in the root canal with smaller ones.

The advantages included more accurate working length determination (Stabholz et al. 1995). The rotary movement also augered the majority of the debris coronally and thus resulted in less apical debris extrusion out of the apical end of the root (Kustarci et al., 2008). The properties inherent to NiTi instruments also meant that they tend to stay centered in the canal much better when compared to stainless steel files (Kuhn et al., 1997). While all files have a tendency to transport root canals, NiTi instruments cause significantly less transportation (Coleman et al., 1997).

Despite their advantages, NiTi instruments can still cause procedural errors if the clinician misuses them. According to Weine et al. (1975), misuse can cause transportation, zipping, ledging, and perforation. Their study found that due to the nature of files to straighten themselves out inside a canal, this can result in alteration of the original curvature (transportation), widening of the apex towards to the outer curvature (zipping), and creating a false exit (perforation). Transportation and perforation are complications that usually start out as a ledge or iatrogencially created root canal irregularity that makes instrumentation to the apex very difficult.

Rotary file designs (K3)

Part of the advantages of the K3 file system is the presence of 3 radial lands to allow for loading of the flutes. This supposedly increases the instrument's resistance fracture through a higher peripheral mass (Schafer et al.,

2003). The asymmetrical cross section of the K3 files functions to reduce the contact area between these radial lands and the canal wall and also decrease frictional resistance (Bergman et al., 2001)

The self-centering ability of K3 files was demonstrated by Yoshimine et al. (2005) in the instrumentation of S-shaped acrylic resin block. When compared to Protaper files, K3 files were less likely to cause apical zipping and ledging while maintaining the original curvature of the simulated canals. The addition of the variable helical flute angle design helps facilitate debris movement coronally and prevents clogging of the instrument (Gambarini 2005). In a study that compared K3 files against both Profiles and RaCe files, the progressively deeper flutes found along the length of the file was one reason that K3 files exhibited more resistance to cyclic failure than the latter two. The reason given was a slower increase in the thickness of the metal core which increased overall flexibility of the instrument (Yao et al., 2006).

Positive rake angle

The rake angle is described by Chow et al. (2005) as the angle between two lines. The first line (peripheral line) is drawn between the cutting tip and center of the instrument while the second one lies at a tangent to the curve of the cutting surface's tip. A positive rake angle is defined as the location of the peripheral line in front of the cutting surface while the opposite is true for the negative rake angle. The positive rake angle allows the flutes of the file to directly

engage against the cutting surface. The result is a more efficient cutting motion as opposed to a scraping motion produced by instruments with a negative rake angle (Bergmans et al., 2003).

Due to the presence of this feature, curved canals in acrylic resins were prepared more rapidly with few canal aberrations and minimal transportation towards the outer aspects of the curve. However, the more aggressive cutting action also resulted in an increased risk of instrument separation since the files have a tendency to bind to the canal walls (Schafer et al., 2003).

Non-cutting tip

Another feature of the K3 files is the presence of a non-cutting tip (Gambarini, 2005). The Non-cutting tip design was first described by Wildey et al. (1992) as being rounded when compared to the inclined plane that was present on a cutting tip. This makes the instrument less likely to cut against the outer curve of the canal and thus minimizes procedural errors such as ledging, zipping, canal transportation, and perforation (Gambarini 2005).

Added flexibility

Structurally, the heat treatment received by K3 files enables it to undergo an intermediate phase called the R-Phase. The R-Phase was first described Kuhn et al. (2002) as an intermediate phase between the austenitic to martensitic transformation. Due to its lower Young's modulus, the material in this phase is actually more flexible when compare to its martensite form.

Taper size

Larger apical preparations were found to have a positive correlation with canal cleanliness. Usman et al. (2004) compared apical preparation of GT file size 20 and 40 (both at .06 taper) and found that significantly more debris were left in the apical third when the canal was instrumented to a GT size 20. Alternatively, larger canal preparations can compromise root structure. Haikel et al. (1999) also found that as the taper size of the instrument increases, time to instrumentfracture decreases.

Root fractures and RCT

It was previously established that the majority of vertical root fractures (VRF) are usually associated with endodontically treated teeth and the incidence was found to be as high as 67% in molars (Gher et al., 1987). The results from Cohen et al. (2003) strengthened this association when they found that in 36 specimens with VRF, 34 (94%) had been endodontically treated and up to 91%

of the VRF were due to inadequately designed dowels or inappropriate selections of tooth for abutment. According to Meister et al. (1980), excessive force exerted during compaction of gutta-percha was the main cause 84% of the time. Other causes included operative related errors/incorrect post space preparation. During obturation, the main culprit is excessive amount of spreader load while compacting of gutta percha. Holcomb et al. (1987) discovered a positive linear correlation between fracture load and root width, canal width, canal taper, ratio of canal width and the number of accessory cones placed. Additionally, improperly prepared spreader placement may also result in unnecessary apical forces and possible root fracture.

Histologically, Walton et al. (1984) found that fractures confined to the root or initiated apically were usually in the buccolingual direction while mesial-distal fractures originated within the crown. Bacteria, food debris, obturation materials were commonly found in the fracture space surrounded by granulomatous tissue and resorption of the supporting bone. A fracture line created a continuous pathway for microorganisms to enter from the oral environment into the canal and persisted as a source of chronic inflammation for as long as the affected tooth still remains. Tamse et al. (2006) found that clinical presentations of VRF included: percussion sensitivity, fenestration or dehiscence in the alveolar bone and also linked intraradicular dowels/posts as a possible cause. The challenge presented in diagnosis of these root fractures is that many had symptoms that are similar to that of failing root canal therapy. Specifically, Testori et al.(1993) investigated 36 cases of VRF and found that 78% contained a periodontal

pocket, 72% had apical radiolucency associated with the affected area, swelling was present in 53% of all cases, and 42% had a sinus tract. Unfortunately in many of these cases, the confirmation of vertical root fracture diagnosis was not made until about 10.8 years after the original endodontic treatment was completed.

Many of these vertical fractures can also start out as craze lines or incomplete fracture at the time of instrumentation. Bier et al. (2009) found that in a comparison test of hand instrumentation versus different rotary instrument systems, the aforementioned defects were only detected on root sections that had been instrumented with GT (4%), Profile (8%), or Protaper (16%) rotary files. Wilcox et al. (1997) stated that those defects could then progress into vertical root fractures when the teeth are subjected to additional stresses from possible retreatment procedures or normal mastication and therefore the accumulation of stress over a lifetime may be the most significant factor affecting the incidence of root fracture. Using a different approach to determine the pattern of stress on the root structure, Rundquist et al. (2006) used a finite element analysis model that utilizes computer simulation to generate stress pattern on a premolar during simulated obturation and masticatory loading. It was interesting to note that in their research, an increased taper tended to decrease stress during obturation but had the opposite effect when it came to mastication. The former procedure tended to create the most stress on the canal surface while the latter transferred the majority of this load onto the external root surface. Aside from obturation and instrumentation, the medicaments and irrigants (such as mineral trioxide

aggregate (MTA), calcium hydroxide (CaOH2), and sodium hypochlorite (NaOCl)) that are used during root canal treatment can also negatively impact root dentin. Using bovine root sections, White et al. (2002) found that 5 weeks of exposure to these materials led to a 32 % decrease in root dentin strength for CaOH2, 33% decrease for MTA, and 59% decrease for NaOCl.

Ultimately, fracture susceptibility is intrinsic to the tooth and canal morphology and beyond the influence of the clinician. Canal preparations that are as conservative as possible and rounded in shape will help to eliminate stress concentration sites that can lead to a higher incidence of vertical root fracture. (Sathorn et al., 2005). Previous literature had compared the stress of endodontic procedures versus restorative procedures utilizing occlusal loading. Using a strain gauge that was bonded to the enamel above the cementoenamel junction, Reeh et al. (1989) loaded and unloaded 37 Newtons for 3 seconds on tooth specimens to measure stiffness after being subjected to different dental procedures including access preparation, instrumentation, obturation, MOD preparations, and one and two surface cavity preparation. They found that when it came to endodontic procedure, there was only a 5% loss in tooth stiffness compared to the 63% loss incurred by preparing a MOD cavity preparation. The significance of their results was that the main contributor to loss in tooth stiffness was the presence or absence of intact marginal ridges. Although there is no direct relationship between the significance of this study and the causes of VRF, it is no doubt that large pre-existing restorative work contributes to the overall

amount of stress that a tooth is subjected too during its lifetime prior to endodontic treatment.

A more recent investigation by Sedgley et al. in 1992 attempted to directly compare the change in tooth structure between endodontically treated and vital teeth. By using extracted matched pair teeth, the biomechanical properties (punch shear strength, toughness, load to fracture, and microhardness) were evaluated to determine the differences with vital versus nonvital tooth structure. For their load to fracture test, the roots were standardized and a mounting jig on an Instron machine was used to load the coronal face of the specimens. The crosshead speed at which the jig was advancing at was .1 mm/min. At the conclusion of all the testing, they found no difference between the biomechanical properties of vital versus endodontically treated teeth. There were, however, some drawbacks in their study design. First, there may have been some thermal and mechanical damage that was inadvertently created during preparation of the specimens. As with many *in vitro* studies, this is a common problem. Extended storage time of the specimens (up to three months) did not seem have an effect on the results although the authors did point out that this was limited to the types of testing in their study. Other inadequacies regarding the details of this study include tooth types that were never specified, the effects of tooth morphology on fracture properties was not taken into account, and there were no attempts made to quantify the specific instrumentation technique that was used in the endodontic treatment. The size of the endodontic preparation, as previously stated, can have an effect on dentinal strength. By loading the coronal portion of the root, the

study relied solely on the transfer of force in a coronal to apical direction and does not evaluate whether there was a different effect between the apical, middle, and coronal region of the same root.

Purpose

This research attempts to address the following questions:

1. Does increasing taper size lead to a decrease in load fracture resistance within the root structure?
2. Is there a difference in load fracture resistance within different regions of the same root?

Null Hypothesis

The null hypothesis states that there are no differences in fracture resistance between the three taper sizes.

Materials and Methods

Specimen selection and sample size included 36 extracted single rooted lower premolars stored in 0.05% sodium azide. Each individual specimen was inspected for fractures and excluded from the study if root caries, multiple canals, signs of root fracture/root defects, and open apices were present. The teeth were accessed with a Transmetal bur (Dentsply Maillefer, Tulsa, OK) and size 10 K files (Dentsply Maillefer, Tulsa, OK) were used to determine the canal length and working length was set at 1 mm short of the apical foramen as described by Sathorn et al. (2005). The specimens were randomized using an online random number generator and divided into three groups (.02, .04, and .06 taper). Determination of the control for this study was based on an earlier pilot study. The teeth were then instrumented using a crown down technique following manufacturer's instructions using the Aseptico Surgimotor II torque control motor (Dentsply, Tulsa, OK) set at 350 rpm (manufacturer's recommended speed). K3 files (SybronEndo, Orange, CA) were used for the 3 taper groups. The files sequence for this technique was as followed: 25 .12 file, 25 .10 file, 25 .08 file, 25 .06 file, 25 .04 file. The addition of a 25 .02 file was necessary to maintain proper taper throughout the canals of the teeth within the control group (.02 taper). All the specimens were apically enlarged up to a size 35 K3 file with a different taper (.02, .04, .06) depending on the group they were assigned to. 5.25% NaOCl was used as an irrigant in between files and this was delivered with a Maxi Probe tip. The specimens were held in place using a holding jig and Integrity (Dentsply,

Tulsa, OK) was flowed into the surrounding area to create a mold, which facilitated mounting of the specimen on the Isomet Low Speed Saw (Buehler, Lake Bluff, IL). To standardize the root sections, 2 mm was sectioned off from each root apex. After standardization of the specimens, 2 mm thick sections were cut to produce a total of 4 sections per specimen. The 2 mm sections were determined based on a pilot study which found the most consistent reading when loaded to fracture on the MTS machine. Three separate Tungsten rods were made to replicate the different tapers. These rods are mounted on the crosshead of the MTS 858 machine (MTS, Eden Praire, MN) to load the root sections until they are fractured. Prior to the loading test, the individual root sections were photographed on a standard mm ruler from both the apical and coronal aspect to determine surface area. The sections were then placed in a holder directly below the crosshead and loaded to fracture at a constant rate of .2 mm/min. The point at which the root sections fractured was determined by an audible cracking sound and confirmed with a fiber optic light. The machine was programmed to record the maximum force loaded onto each individual root section. Using ImageJ software (NIH, Bethesda, MD) downloaded from the NIH website, the photo image of both the coronal and apical aspect of each root section was measured using a tracing tool which also converted pixel density into units of mm. The center portion which was instrumented was measured along with the entire root section's surface area. The net surface area was determined after subtracting the area of instrumentation from that of the entire root section. An average value of the surface area was calculated from the apical and coronal

aspect. The value from the load to fracture test was then used to determine a force to surface area ratio. Although steps were taken to ensure consistent root morphology among the specimens, it is inevitable that there will be a range of variability in terms of the shape of each root section. To standardize this, it was more comparable to use the ratio of the load to surface to area rather than just the values from the load to fracture test alone.

Figure 1A

Figure 1B

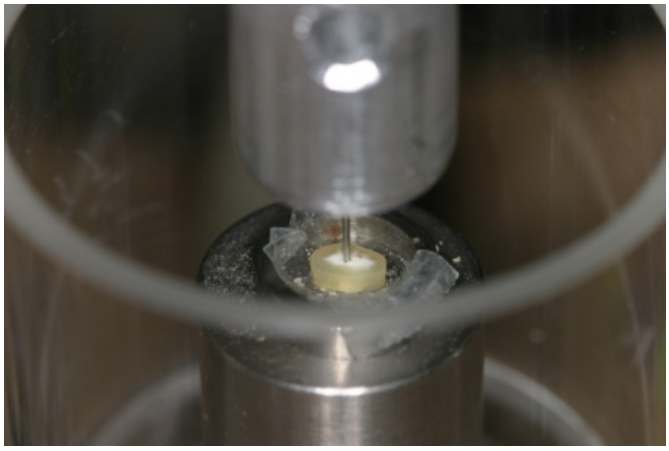

Figure 2A

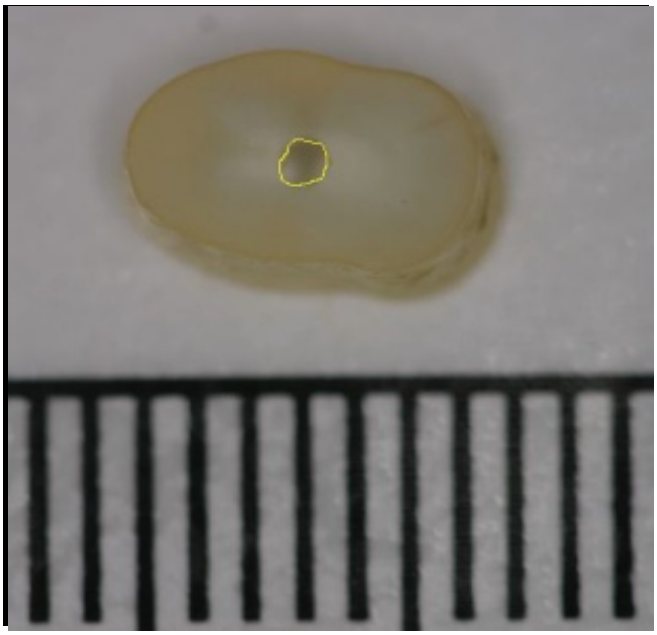

Figure 2B

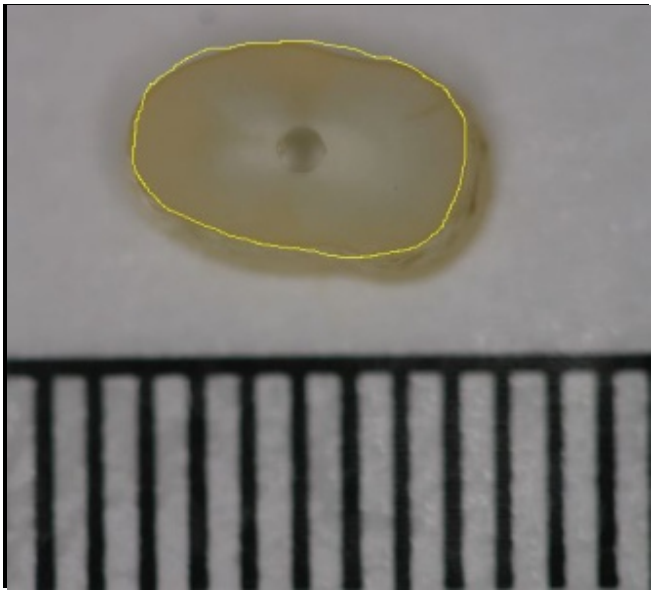

Results

The results for each specimen are listed in the following table that records the average surface area, load to fracture, and load to area ratio that was calculated based on the distance from the anatomical apex of the root section.

Table 1. Distance from apex, average surface area, load to fracture, and load to area ratio.

Group A	Group B	Group C
.04 Taper	.06 Taper	.02 Taper
Specimen 1-12 (A1-A12)	Specimen 1-12 (B1-B12)	Specimen 1-12 (C1-C12)

Specimen A1	Avg. Surface Area	Load to Fracture	Load to Area Ratio
2 mm from apex	28.988	130.764	4.511
4.5 mm from apex	39.755	160.411	4.035
7 mm from apex	48.362	121.872	2.52
9.5 mm from apex	69.504	168.686	2.427

Specimen A2	Avg. Surface Area	Load to Fracture	Load to Area Ratio
2 mm from apex	28.612	130.070	4.546
4.5 mm from apex	53.368	131	2.461
7 mm from apex	53.980	97.380	1.804
9.5 mm from apex	66.660	91.324	1.370

Specimen A3	Avg. Surface Area	Load to Fracture	Load to Area Ratio
2 mm from apex	20.081	31.266	1.557
4.5 mm from apex	38.398	72.227	1.881
7 mm from apex	50.184	94.998	1.893
9.5 mm from apex	69.065	113.267	1.64

Specimen A4	Avg. Surface Area	Load to Fracture	Load to Area Ratio
2 mm from apex	22.96	57.584	2.508
4.5 mm from apex	29.744	80.725	2.714
7 mm from apex	38.278	64.154	1.676
9.5 mm from apex	44.947	68.634	1.527

Specimen A5	Avg. Surface Area	Load to Fracture	Load to Area Ratio
2 mm from apex	28.340	122.882	4.336
4.5 mm from apex	38.191	194.545	5.094
7 mm from apex	43.720	215.846	4.937
9.5 mm from apex	56.070	185.143	3.302

Specimen A6	Avg. Surface Area	Load to Fracture	Load to Area Ratio
2 mm from apex	37.516	25.661	.684
4.5 mm from apex	42.228	92.310	2.186
7 mm from apex	48.511	196.512	4.051
9.5 mm from apex	54.426	113.097	2.078

Specimen A7	Avg. Surface Area	Load to Fracture	Load to Area Ratio
2 mm from apex	31.710	74.867	2.361
4.5 mm from apex	62.391	105.753	1.695
7 mm from apex	76.342	134.515	1.762
9.5 mm from apex	79.836	93.887	1.176

Specimen A8	Avg. Surface Area	Load to Fracture	Load to Area Ratio
2 mm from apex	39.598	165.322	4.175
4.5 mm from apex	71.222	103.557	1.454
7 mm from apex	76.802	116.509	1.517
9.5 mm from apex	92.234	116.584	1.264

Specimen A9	Avg. Surface Area	Load to Fracture	Load to Area Ratio
2 mm from apex	33.016	71.678	2.171
4.5 mm from apex	56.470	80.583	1.427
7 mm from apex	74.244	101.194	1.363
9.5 mm from apex	90.020	82.458	.916

Specimen A10	Avg. Surface Area	Load to Fracture	Load to Area Ratio
2 mm from apex	31.232	79.834	2.268
4.5 mm from apex	57.381	69.316	1.208
7 mm from apex	78.720	50.381	.64
9.5 mm from apex	90.678	47.606	.525

Specimen A11	Avg. Surface Area	Load to Fracture	Load to Area Ratio
2 mm from apex	33.374	66.481	1.992
4.5 mm from apex	61.612	77.015	1.25
7 mm from apex	71.542	41.566	.581
9.5 mm from apex	78.794	60.750	.771

Specimen A12	Avg. Surface Area	Load to Fracture	Load to Area Ratio
2 mm from apex	48.586	88.621	1.824
4.5 mm from apex	67.050	138.794	2.070
7 mm from apex	90.444	69.009	.763
9.5 mm from apex	112.832	89.814	.796

Specimen B1	Avg. Surface Area	Load to Fracture	Load to Area Ratio
2 mm from apex	22.934	90.291	3.937
4.5 mm from apex	51.644	120.537	2.334
7 mm from apex	60.196	130.625	2.170
9.5 mm from apex	84.538	56.387	.667

Specimen B2	Avg. Surface Area	Load to Fracture	Load to Area Ratio
2 mm from apex	39.154	107.516	2.746
4.5 mm from apex	46.291	134.113	3.741
7 mm from apex	57.482	71.673	.802
9.5 mm from apex	60.424	153.416	2.539

Specimen B3	Avg. Surface Area	Load to Fracture	Load to Area Ratio
2 mm from apex	67.054	104.404	4.645
4.5 mm from apex	37.164	69.905	3.616
7 mm from apex	50.541	95.675	1.493
9.5 mm from apex	79.775	130.831	.916

Specimen B4	Avg. Surface Area	Load to Fracture	Load to Area Ratio
2 mm from apex	18.161	130.015	7.159

4.5 mm from apex	34.492	102.235	2.964
7 mm from apex	35.279	63.784	1.808
9.5 mm from apex	44.492	122.532	2.754

Specimen B5	Avg. Surface Area	Load to Fracture	Load to Area Ratio
2 mm from apex	20.191	130.253	6.451
4.5 mm from apex	28.764	82.583	2.871
7 mm from apex	42.592	45.488	1.068
9.5 mm from apex	51.744	41.292	.798

Specimen B6	Avg. Surface Area	Load to Fracture	Load to Area Ratio
2 mm from apex	22.050	64.959	2.946
4.5 mm from apex	38.088	46.125	1.211
7 mm from apex	50.942	49.516	.972
9.5 mm from apex	61.786	51.530	.834

Specimen B7	Avg. Surface Area	Load to Fracture	Load to Area Ratio
2 mm from apex	38.626	86.444	2.238
4.5 mm from apex	54.545	128.071	2.348
7 mm from apex	62.325	132.939	2.133
9.5 mm from apex	67.674	72.344	1.069

Specimen B8	Avg. Surface Area	Load to Fracture	Load to Area Ratio
2 mm from apex	39.781	107.090	2.692
4.5 mm from apex	45.368	82.751	1.824
7 mm from apex	57.588	57.070	.991
9.5 mm from apex	74.061	84.430	1.140

Specimen B9	Avg. Surface Area	Load to Fracture	Load to Area Ratio
2 mm from apex	30.499	71.337	2.339
4.5 mm from apex	40.486	70.162	1.733
7 mm from apex	51.580	83.354	1.616
9.5 mm from apex	67.279	82.080	1.22

Specimen B10	Avg. Surface Area	Load to Fracture	Load to Area Ratio

2 mm from apex	40.234	80.629	2.004
4.5 mm from apex	49.354	125.889	2.551
7 mm from apex	61.543	183.462	2.981
9.5 mm from apex	75.499	130.085	1.723

Specimen B11	Avg. Surface Area	Load to Fracture	Load to Area Ratio
2 mm from apex	26.832	66.302	2.471
4.5 mm from apex	44.327	85.772	1.935
7 mm from apex	53.485	99.536	1.861
9.5 mm from apex	60.052	82.751	1.378

Specimen B12	Avg. Surface Area	Load to Fracture	Load to Area Ratio
2 mm from apex	36.047	121.189	3.362
4.5 mm from apex	43.317	51.027	1.178
7 mm from apex	56.922	62.273	1.094
9.5 mm from apex	72.223	90.640	1.255

Specimen C1	Avg. Surface Area	Load to Fracture	Load to Area Ratio
2 mm from apex	39.311	97.186	2.472
4.5 mm from apex	57.322	44.145	.770
7 mm from apex	59.35	51.53	.868
9.5 mm from apex	67.190	40.146	.957

Specimen C2	Avg. Surface Area	Load to Fracture	Load to Area Ratio
2 mm from apex	18.490	48.706	2.634
4.5 mm from apex	32.630	76.756	2.352
7 mm from apex	46.295	37.263	.805
9.5 mm from apex	59.319	64.623	1.089

Specimen C3	Avg. Surface Area	Load to Fracture	Load to Area Ratio
2 mm from apex	21.493	41.627	1.937
4.5 mm from apex	40.477	37.934	.937
7 mm from apex	57.704	56.566	.980
9.5 mm from apex	60.529	36.760	.607

Specimen C4	Avg. Surface Area	Load to Fracture	Load to Area

			Ratio
2 mm from apex	30.344	44.984	1.483
4.5 mm from apex	37.993	60.932	1.604
7 mm from apex	46.792	52.873	1.13
9.5 mm from apex	65.821	64.119	.974

Specimen C5	Avg. Surface Area	Load to Fracture	Load to Area Ratio
2 mm from apex	41.502	53.209	1.282
4.5 mm from apex	51.688	54.552	1.055
7 mm from apex	71.390	68.819	.963
9.5 mm from apex	90.798	38.152	.420

Specimen C6	Avg. Surface Area	Load to Fracture	Load to Area Ratio
2 mm from apex	53.434	30.885	.578
4.5 mm from apex	70.291	40.956	.583
7 mm from apex	89.512	60.930	.681
9.5 mm from apex	100.792	33.405	.331

Specimen C7	Avg. Surface Area	Load to Fracture	Load to Area Ratio
2 mm from apex	37.583	57.067	1.512
4.5 mm from apex	58.320	95.172	1.632
7 mm from apex	72.152	60.930	.844
9.5 mm from apex	98.822	79.900	.808

Specimen C8	Avg. Surface Area	Load to Fracture	Load to Area Ratio
2 mm from apex	58.641	45.152	.770
4.5 mm from apex	67.672	60.762	.898
7 mm from apex	89.352	73.015	.817
9.5 mm from apex	106.745	122.364	1.146

Specimen C9	Avg. Surface Area	Load to Fracture	Load to Area Ratio
2 mm from apex	44.847	97.013	2.181
4.5 mm from apex	60.112	56.566	.941
7 mm from apex	72.596	64.791	.892
9.5 mm from apex	94.381	66.134	.701

Specimen C10	Avg. Surface Area	Load to Fracture	Load to Area

			Ratio
2 mm from apex	41.539	50.859	1.224
4.5 mm from apex	61.79	94.165	1.524
7 mm from apex	64.353	48.174	.749
9.5 mm from apex	79.418	21.821	.275

Specimen C11	Avg. Surface Area	Load to Fracture	Load to Area Ratio
2 mm from apex	41.828	77.044	1.842
4.5 mm from apex	70.524	75.200	.763
7 mm from apex	83.424	80.737	1.066
9.5 mm from apex	98.748	75.366	.968

Specimen C12	Avg. Surface Area	Load to Fracture	Load to Area Ratio
2 mm from apex	27.170	40.788	1.501
4.5 mm from apex	43.686	71.169	1.629
7 mm from apex	66.660	82.080	1.353
9.5 mm from apex	72.780	61.770	.849

Statistical Analysis

Descriptive statistics were calculated for the Load to Fracture to Area ratios for each taper group. Analysis of variance (ANOVA) was used to compare the group means for each root section. If the overall ANOVA was significant ($p < 0.05$), pairwise comparisons were made using a Tukey-Kramer adjustment. A random intercept model was used to compare root section means within each group. P-values less than 0.05 were considered statistically significant. SAS V9.1.3 (SAS Institute Inc, Cary, NC) was used for the analysis.

Table 2. Descriptive Statistics for Load to Fracture to Area ratios

Taper	Distance from Apex	N	Mean	Std Dev	Median	Minimum	Maximum
0.02	2 MM	1	1.62	0.63	1.51	0.58	2.63
	4.5 MM	2	1.22	0.52	1.00	0.58	2.35
	7 MM	1	0.93	0.19	0.88	0.68	1.35
	9.5 MM	2	0.76	0.29	0.83	0.28	1.15
		1					
		2					
		1					
		2					
0.04	2 MM	1	2.74	1.31	2.31	0.68	4.55
	4.5 MM	2	2.29	1.18	1.98	1.21	5.09
	7 MM	1	1.96	1.33	1.72	0.58	4.94
	9.5 MM	2	1.48	0.80	1.32	0.53	3.30
		1					
		2					
		1					
		2					
0.06	2 MM	1	3.58	1.69	2.85	2.00	7.16
	4.5 MM	2	2.36	0.84	2.34	1.18	3.74
	7 MM	1	1.58	0.65	1.55	0.80	2.98
	9.5 MM	2	1.36	0.67	1.18	0.67	2.75
		1					
		2					
		1					
		2					

Table 3. Pairwise Spearman Correlation Coefficients of Root Sections

N=36	2 MM	4.5 MM	7 MM
2 MM	1		
4.5 MM	0.57	1	
7 MM	0.35	0.57	1
9.5 MM	0.40	0.59	0.66

Table 4. One-way ANOVAs Comparing Mean Load to Fracture to Area Ratios between Groups (.02, .04, and .06 taper)

Distance from Apex	P-value
2 MM	0.0028†
4.5 MM	0.0054††
7 MM	0.0198†††
9.5 MM	0.0172‡

† 0.02 vs 0.06 is statistically significantly different (p=0.0019)

†† 0.02 vs 0.04 and 0.02 vs 0.06 are statistically significantly different (p=0.0162 and p=0.0100, respectively)

††† 0.02 vs 0.04 is statistically significantly different (p=0.0159)

‡ 0.02 vs 0.04 is statistically significantly different (p=0.0204)

Since the root sections of the same root appear to be correlated (see Table 2), this was taken into account when comparing root sections within each taper group using the random intercept model.

Table 5. Random Intercept Models

Taper	Type 3 Test for Root Section Effect
0.02	p<0.0001†
0.04	p=0.0029††
0.06	p<0.0001†††

† 2 mm vs 7 mm, 2 mm vs 9.5 mm and 4.5 mm vs 9 mm are statistically significantly different (p=0.0007, p<0.0001 p=0.0303, respectively

†† 2 mm vs 9.5 mm is statistically significantly different (p=0.0018)

††† 2 mm vs 7 mm and 2 mm vs 9.5 mm are statistically significantly different (p=0.0001 and p<0.0001, respectively)

Discussion

Through prior studies, it was shown that microorganisms were the etiology of pulpal and apical inflammation (Kakehashi et al., 1965, Moller et al. 1981). The goal of endodontic therapy is the removal of infected/necrotic pulp tissue, microorganisms and endotoxin from the root canal system to facilitate healing. According to Schilder (1974), these are the biological objectives of cleaning and shaping of the canal; in order to achieve this, the mechanical objectives of cleaning and shaping root canals must be established through a preparation that has a continuously tapering shape which becomes wider in the coronal aspect, occupies as many planes as possible while mimicking the original shape of the canal, and preserves the size and location of the apical foramen. As described by Siquiera et al. (1999), instrumentation alone can remove up to 90% of all microorganisms from the root canal system. W.F. Buehler's discovery of NiTi revolutionized the construction and designs of endodontic files and established rotary instrumentation as the new standard in carrying out the principles set forth by Dr. Schilder. The advantages of NiTi as a material in endodontics were discussed by Thompson (1999), which included a superelastic phase that occurred during the Austenitic to Martensitic transformation and the ability to undergo recoverable deformation. When used as a material in rotary files, Kustarci et al. (2008) found less apical extrusion of debris, better centering ability as demonstrated by Kuhn et al. (1997) and a decrease in the degree of canal transportation was seen in the study by Coleman et al. (1997) when compared to

hand filing. Whether hand or rotary instrumentation is used, it must be kept in mind that all canal instrumentation techniques will inevitably weaken the root structure. The incidence of vertical root fracture had historically been linked to endodontically treated teeth by Gher et al. (1997) and Cohen et al. (2003). Tamse et al (2006) indicated that signs and symptoms of vertical root fractures included percussion sensitivity due to the egress of microorganism into these fracture lines and results in inflammation of the periodontium and subsequent alveolar bone loss. Due to the nature of its complicated diagnosis, root fractures often go undiagnosed for over 10 years on average post-treatment. The primary factor, according to Holcomb et al. in causing and initiating vertical root fracture was excessive spreader load. Additional factors included defects created during rotary instrumentation (forming craze lines or incomplete fractures), and the use of NaOCl, MTA, and CaOH2. Regardless of the factors that are involved in vertical root fractures, it is prudent for practitioners to be as conservative as possible when performing root canal therapy to minimize the risks.

This study evaluated the effects of taper sizes on the fracture resistance of root sections and investigated differences within the same root. Single-rooted mandibular premolars were accessed and instrumented with K3 files of different tapers (.02, .04, and .06). K3 rotary files were used in this study due to their standardized taper, which facilitated the fabrication of the mounting jig used in the MTS machine and ensured an even distribution of forces on the root sections. All the specimens were apically enlarged to a master apical file size of

35. The decision to use this size was based on the irrigation needle tip size since Maxi Probe tips, with a diameter size of .31 mm, were used to deliver the 5.25% NaOCl irrigant. The specimens were then mounted in a mold made from Integrity temporary crown material and 2 mm of the apical root was sectioned off. The 2 mm was determined based on past studies by Kuttler et al. (1955) that looked at the anatomical apex and the major and minor diameter. The results showed that on average, the distance between the anatomic apex and the minor diameter/minor constriction was found to range from 1.019 mm to 1.266 mm from the apex depending on the age group. A more recent study by Stein et al. (1990) found this distance to be 1.2 mm on average. Since the goal is to end the preparation at the minor constriction/cementoenamel junction, the 2 mm resections ensured that we are close to this area. Cross sectioning the root eliminated the variability of canal curvature which could have a significant influence on fracture susceptibility (Lertchirakarn et al., 2003). Another added benefit using this preparation method was the ability to minimize canal irregularities since stress tended to concentrate at the tip of these defects (Callister et. 2003). The sections were then photographed and subjected to the load to fracture test using jigs that were made to resemble the corresponding file and taper size mounted on the MTS machine. The .2 mm/crosshead speed that was used to advance the jig was based on past studies which utilized a range from .1 mm/min to .2 mm/min (Sedgeley et al.; 1992, Chen et al.; 2011). A pilot study conducted prior to this experiment found no differences between the two speeds. At the same time, the cross sections of each root were photographed

and the surface area was calculated. Since there is so much variations in the anatomy of each individual roots, it was determined that a ratio of the force required to fracture the specimen and the corresponding surface area might give a more accurate assessment since it accounts for the relative size differences of each sections. In this study, the force to root ratio tended to decrease coronally in the cross sections. A surprising trend in the results was that the average load to area ratio was highest among the .06 taper group in the 2 mm and 4.5 mm region at 3.58 N/mm2 and 2.36 N/mm2, respectively while it was the lowest in the .02 taper group at 1.62 N/mm2 and 1.22 N/mm2, respectively. This could be explained by the uneven distribution of forces on the canal walls due to the minimal preparation in the .02 taper group. In the larger taper groups, the larger preparation sizes might have allowed better force distribution and hence the higher ratios. When comparing the individual root sections within the same specimen, the general trends showed that the ratio tended to decrease as we advance coronally. One explanation might be the present of canal irregularities that remained in the coronal portion of the roots where uneven forces could concentrate (Callister et al. 2003) and caused a premature fracture to form. The under preparation of the .02 taper group also made this more apparent as significant differences were found in the ratios between the sections that were 2 mm away from the apex compared to the more coronal regions (7 mm and 9 mm away from the apex).

According to the data within the results, it was found that the larger the preparation, the higher the force needed to fracture the root section. Therefore, it appeared that a positive correlation existed between increasing taper size and higher force to surface area ratio. Since the force to area ratios also appeared to be higher in the apical region compared to the coronal portion, this might indicate better force distribution when the specimens are subjected to a spreader like force the closer the preparation is to the apex. The results also indicated that while larger preparations may empirically weaken root structure, it may eliminate more canal irregularities that can lead to more favorable force distribution laterally.

Previous literature has only compared the biological properties of vital teeth to endodontically treated teeth. Very few studies have looked at varying taper size and their effect on the root's fracture resistance. This study used root sections instead of the whole root, which was the case in previous studies. Since buccolingual fractures were confined to the root and initiated apically (Walton et al., 1984), cross sections of the root may be able to better determine if instrumentation with different tapered files is the primary cause. By sectioning the roots, it was possible to study the behavior of each area in the root canal when it was subjected to a spreader-like force. It does reiterate Lertchirakarn et al.'s findings in 2003 that a more rounded canal preparation does a better job in distributing stresses evenly and minimizing stress concentration areas. The application of forces laterally may only be one way in which vertical root fractures

are formed. This study also indirectly confirmed Rundquist et al.'s (2005) findings that indicated decreased root stresses in larger taper preparations when subjected to compaction forces.

This study utilized a jig that was fabricated to resemble the file used in the instrumentation process, this is the first of its kind to use this particular method of evaluation. Sedgeley et al. (1992) used a jig to perform the load to fracture test but that was on an entire root and the comparison was vital versus endodontically treated teeth. No studies have compared taper size extensively and attempted to draw a comparison regarding increasing taper sizes and the root fracture resistance between different regions of the root itself.

Although this study attempted to form a link between susceptibility to vertical root fracture when comparing instruments of different taper sizes, the results left more questions than answers as to identifying specific factors that might play a role in causing vertical root fracture in endodontically treated teeth. One of the drawbacks in this study was that while using root sections instead of the whole root can eliminate the effect of canal curvature on stress concentration, this is one of the most important factor when it comes to stress distribution according to Lertchirakarn et al. (2003), even more so than external root morphology. Although the point of using standardized taper rotary instrument was to minimize the amount of canal irregularities (Callister et al., 2003) and diminish their effect on the final results, it was evident from the control group (.02 taper) that this accounted for the lower fracture load to surface area ratios. Due

to the unknown extraoral time that each specimen spent in the storage solution, it was difficult to identify whether this may have played a significant role in the final results. Sedgeley et al. (1992) stated that extended storage (up to three months) of specimens did not have a significant difference whereas Huang et al. (1992) indicated that the moisture contents of teeth within the mouth and the ones that are extracted are vastly different and the preparation of specimen will cause some form of dehydration, which can lead to different behavioral characteristics of the dentin itself. Furthermore, the mesiodistal fracture patterns of some of the specimens within the study were not consistent with what Walton et al. (1984) found in vertical root fractures that were initiated apically. It would be difficult to ascertain whether or not the force applied during this study resembled what is occurring in an *in vivo* situation. There was also a large range in the standard deviations across multiple data groups within this study (.19-1.69), this can be explained by the variations in the canal morphology/irregularities shown by Callister et al. (2003) from specimen to specimen even though standardized rotary files were used for the instrumentation process. Another factor that could account for such a large range for the standard deviation is the fact that during the process of specimen preparation, there could have been mechanical and thermal damages to root structure. Sedgeley et al. (1992) concluded that this can have an effect in the biomechanical testing of dentin. Every attempt was made to inspect the root structures of all specimens for signs of fracture, craze lines, and caries, however, potential microscopic fractures could not be verified.

This was a novel attempt to elucidate on the role that different taper sizes might have on the fracture resistance of root sections and explore the possible link of taper sizes and the incidence of vertical root fracture. Due to the nature of the testing apparatus, it would be interesting to see if similar results are obtained from future studies that might opt to perform the testing with submerged specimens. Every attempt was made to design a control group that would yield comparable results. It is also possible that the material of choice within the jig itself can also play a factor, as different metals exhibit different characteristics when subjected to stress. The anatomic variation between different specimens makes this an extremely difficult task. As advocated in past studies including Sathorn et al. (2003), it is still prudent to conserve as much tooth structure as possible since the stress over time can have an additive effect on the root and many other factors (mastication forces, post placement, beside instrumentation size, some beyond the control of the clinician, can play a role in inducing vertical root fractures in endodontically treated teeth.

Within the limited scope of this study, it can be concluded that larger taper size increases the load to fracture resistance within the root structures and that there was a difference in the load to fracture between different areas of the same root, with the more apical region exhibiting a higher load to fracture resistance and thus the null hypothesis is rejected.

Conclusion

Since its inception, the discipline of endodontics has evolved and expanded from a field to a specialty; major breakthroughs assisted this change via improved understanding of endodontic infections and instrumentation concepts. Advancements over the years brought forth development of a wide range of endodontic file systems. Despite the significant impact root fractures have on the outcome of root canal therapy, the effects of specific file properties on the risks of root fracture following endodontic treatment remains unclear. In this study we attempted to elucidate the link between increased taper and increased risk of root fractures in sectioned root segments. Taper size appears to be one of many factors which affect the distribution of forces along the root structure. Further investigation of different file system properties and how they influence force distribution will allow us to minimize the risk of root fractures and improve prognosis for endodontically treated teeth.

References

Bier CAS, Shemesh H, Tanomaru-Filho M, Wesselink PR, Wu MK. The ability of different nickel-titanium rotary instruments to induce dentinal damage during root canal preparation.. J Endod 2009;35:236-8.

Bergmans L, Van Cleyenbrugel J, Beullens, Wevers M, Van Meerbeek B, Lambrechts P. Progressive versus constant tapered shaft design using NiTi rotary instruments. Int Endod J 2003;36:288-95.

Card SJ, Sigurdsson A, Orstavik D, Trope M. The effectiveness of increased apical enlargement in reducing intracanal bacteria. J Endod 2002;28:779-83.

Clegg MS, Vertucci FJ, Walker C, Belanger M, Britto LR. The effect of exposure to irrigant solutions on apical dentin biofilms in vitro. J Endod 2006;32:434-7.

Chen YC, Li H, Fok A. In vitro validation of a shape-optimized fiber-reinforced dental bridge. Dent Mat 2011;27:1229-37.

Cohen S, Blanco L, Berman L. Vertical root fractures clinical and radiographic diagnosis. J Am Dent Assoc 2003;134:434-41.

Coleman CL, Svec TA. Analysis of Ni-Ti versus stainless steel instrumentation in resin simulated canals. J Endod 1997;23:232-5.

Cruse WP, Bellizzi R. A historic review of endodontics, 1689-1963, part 1. J Endod 1980;6:496-99.

Gambarini G. The K3 rotary nckel titanium instrument system. Endodontic Topics 2005;10:179-82.

Gher ME, Dunlap RM, Anderson MH, Kuhl LV. Clinical survey of fractured teeth. J Am Dent Assoc 1987;114:174-7.

Grossman LI. Endodontics 1776-1976: a bicentennial history against the background of generl dentistry. J Am Dent Assoc 1976;93:78-87.

Haikel Y, Serfaty R, Bateman G, Senger B, Allemann C. Dynamic and cyclic fatigue of engine-driven rotary nickel-titanium endodontic instruments. J Endod 1999;6:434-40.

Holcomb Q, Pitts DL, Nicholls JI. Further investigation of spreader loads required to cause vertical root fracture during lateral condensation. J Endod 1987;13:277-84.

Huang TJG, Schilder H, Nathanson D. Effects of moisture content and endodontic treatment on some mechanical properties of human dentin. J Endod 1992;18:210-5.

Kakehashi S, Stanley HR, Fitzgerald RJ. The effects of surgical exposures of dental pulps in gern-free and conventional laboratory rats. Oral Surg Oral Med Oral Pathol 1965;20:340-8.

Kuhn WG, Carnes DL, Clement DJ, Walker III WA. Effect of tip design of nickel-titanium and stainless steel files on root canal preparation. J Endod 1997;23:735-8.

Kuhn G, Jordan L. Fatigue and Mechanical Properties of Nickel-Titanium Endodontic Instruments. J Endod 2002;28:716-20.

Levy G. A new method for the automation of endodontic procedures: the canal finder. Chir Dent Fr 1984;54:37-43.

McKelvey AL, Ritchie RO. Fatigue-crack propagation in Nitinol, a shape-memory and superelastic endovascular stent material. J Biomed Mater Res 1999;47:301-8.

Meister F, Lommel TJ, Gerstein H. Diagnosis and possible causes of vertical root fractures. Oral Surg Oral Med Oral Path 1980;49:243-253.

Moller AJR, Fabricius L, Dahlen G, Ohman AE, Heyden G. Influence on periapical tissues of indigenous oral bacteria and necrotic pulp tissue in monkeys. Scand J Dent Res 1981;89:475-84.

Peters OA Schonenberger K, Laib A. Effects of four Ni-Ti preparation techniques on root canal geometry assessed by micro computed tomography. Int Endod J 2001;34:221-30.

Rasmussen KJR. Full-range stress-strain curves for stainless steel alloys (report). University of Sydney 2001; report no. R811.

Reeh ES, Messer HH, Douglas WH. Reduction in tooth stiffness as a result of endodontic and restorative procedures. J Endod 1989;15:512-6.

Rundquist BD, Versluis A. How does canal taper affect root stresses. Int Endod J 2006;39:226-37.

Sathorn C, Palamara JEA, Messer HH. A comparison of the effects of two canal preparation techniques on root fracture susceptibility and fracture pattern. J Endod 2005;31:283-7.

Sathorn C, Palamara JEA, Palamara D, Messer HH. Effect of root canal size and external root surface morphology on fracture susceptibility and pattern: a finite element analysis. J Endod 2005;31:288-92.

Schafer E, Florek H. Efficiency of rotary nickel-titanium K3 instruments compared with stainless steel hand K-Flexofile. Part 1. Shaping ability in simulated curved canals. Int Endod J 2003;35:199-207.

Schilder H. Cleaning and shaping the root canal. Dent Clin North Am 1974;18:269-96.

Schonfeld SE, Greening AB, Glick DH, Frank AL, Simon JH, Herles SM. Endodotoxic activity in periapical lesions. Oral Surg Oral Med Oral Pathol 1982;53:82-7.

Sedgeley CM, Messer HH. Are endodontically treated teeth more brittle? J Endod 1992;18:332-5.

Siqueira JF, Lima KC, Magalhaes FA, Lopes HP, de Uzeda M. Mechanical reduction of bacterial population in the root canal by three instrumentation techniques. J Endod 1999;25:332-5.

Stabholz A, Rothstein I, Torabinejad M. Effect of preflaring on tactile detection of the apical constriction. J Endod 1995;21:92-4.

Tamse A. Iatrogenic vertical root fractures in endodontically treated teeth. Endod Dent Traumatol 1988;4:190-6.

Thompson SA. An overview of nickel-titanium alloys used in dentistry. Int Endod J 2000;33:297-310.

Usman N, Baumgartner JC, Marshall JG. J of Endod 2004;30:110-12.

Vaudt J, Bitter K, Kilbassa AM. Evaluation of rotary root canal instruments in vitro: a review. Endo 2007;1:189-203.

Wilcox LR, Roskelley C, Sutton T. The relationship of root canal enlargement to finger-spreader induced vertical root fracture. J Endod 1997;23:533-34.

Walia H, Brantley WA, Gerstein H. An initial investigation of the bending and torsional properties of Nitinol root canal files. J Endod 1988;14:346-51.

Walton RE, Michelich RJ, Smith GN. The histopathogenesis of vertical root fractures. J Endod 1984;10:48-56.

Weine FS, Kelly RF, Lio PJ. The effect of preparation procedures on original canal shape and on apical foramen shape. J Endod 1975;1:255-62.

Wildey WL, Senia S, Montgomery S. Another look at root canal instrumentation. Oral Surg Oral Med Oral Path Iral Radiol Endod 1992;74:499-507.

Wu MK, Barkis D, Roris A, Wesselink PR. Does the first file to bind correspond to the diameter of the canal in the apical region? Int Endod J 2002;35:264-7.

Yao JH, Schwartz SA, Beeson TJ. Cyclic fatigue of three types of rotary nickel-titanium files in a dynamic model. J Endod 2006;32:55-57.